Properties of Slow-mode Shocks in the Distant (>200 R_e) Geomagnetic Tail

C. M. Ho, B. T. Tsurutani and E. J. Smith

Jet Propulsion Laboratory, California institute of Technology, Pasadena, CA 91109

W. C. Feldman

Los Alamos National Laboratory, Los Alamos, NM 87545

Submitted to Journal of Geophysical Research

February 1, 1995

Revised on October 30, 1995

Second revised on February 12, 1996

Abstract: The two distant ISEE-3 geomagnetic tail passes have been examined to identify all slow-mode shocks present in the data. We find a total of 86 events from 439 plasmasheet/lobe crossings, using five criteria based on relations between the upstream lobe and the downstream plasmasheet magnetic field and plasma measurements . The statistical results of slow-mode shock parameters such as the angle between magnetic field and shock normal, θ_{Bn}, Alfven Mach number along the normal direction, M_{An}, and electron beta, β_e, are calculated and reported. On average, the magnetic field decreases by a factor -2,7, the electron density increases by -1.7, temperature increases by -1.8, and the plasma flow velocity increases by - 3.8 across the shocks, The average upstream θ_{Bn} is -76° while the downstream angle is - 50°. The shocks have an average M_{An} -0.87 along the normal direction, and an upstream β_e -0.04. In the downstream plasmasheet region, the dominant plasma flow associated with the shocks is in the tailward direction with an average speed - 585 km/s. Only a fcw cases of earthward downstream plasma flow have been detected. The slow shocks have thicknesses, on average, of -5380 km (about 7 ion inertial lengths) and an average tilt angle of - ±22.4° between the shock normal and z axis. Using the Petschek slow shock mode], the average location of the neutral lines is located in a range of $\pm 40\ R_e$ from observation sites. About half the slow mode shock events arc detected during southward IMF intervals and half during northward intervals. There is a weak substorm dependence of slow mode shocks and plasmoids, a dependence which is most obvious when $B_z > +2$ nT and $B_z < -2$ nT intervals are intercompared. We see a substorm dependence for plasmasheet/lobe crossings which suggests that the deep tail become more dynamic during substorm intervals. We have also sought the existence of large wavetrains downstream of slow shocks that have been theoretically predicted by Coroniti (1971) and simulation studies, No such wavetrains were observed throughout the two ISEE-3 passes of the distant tail. However, wc do detect some medium amplitude transverse waves in the shock ramp regions. The waves have frequencies and polarizations similar to the plasmasheet boundary layer waves reported by Tsurutani et al. (1 985). The waves present in the shock ramp are also right-hand ion cyclotron waves in the plasma frame. We believe that these waves are generated by the ion beams flowing away from the magnetic merging regions,

1. Introduction

Magnetohydrodynamic (MHD) theory shows that there arc three fundamental wave modes for low-frequency waves and plasma discontinuities [Kennel et al., 1985]. When the upstream plasma flow speed relative to the shock speed is greater than the fast mode speed, a fast-mode shock may exist. Across this discontinuity the plasma speed decreases, as the magnetic field strength increases. The density changes in-phase with the magnetic field strength across the shock, When the plasma flow difference has a value between the fast-mode and intermediate-mode speed, the discontinuity may be an intermediate shock. The magnetic field changes direction, but its magnitude may decrease or increase. If the plasma flow speed difference is less than intermediate-mode speed, but greater than slow-mode speed, this discontinuity may be a slow-mode shock, Across the discontinuity the plasma flow speed increases and the magnetic strength decreases. The density changes out-of-phase with the magnetic field strength across the slow shock. Unlike fast-mode shocks, which have been extensively observed and studied under a variety of plasma conditions and geometries, there have been very few studies for slow-mode shocks. For instance, almost all previous work on slow-mode shocks have been case studies only to determine if the jump conditions satisfy the Rankine-Hugoniot relations, simply to determine if slow shocks exist or not.

Theoretical consideration of steady state reconnection leads to the suggestion that slow-modc shocks arc fundamental to magnetic reconnection in the geomagnetic tail[Petschek, 1964; Sonnerup,1970]. Such shocks result from the steepening of slow-mode waves between the high (lobe) and low (plasmasheet) magnetic field strength regions. S1ow shocks may therefore play an important role in magnetic merging and the transfer of energy stored in the tail magnetic field to the plasmasheet particles and to the creation of energetic particles. The excursions of ISEE-3 into the deep geomagnetic tail have provided direct observational evidence that such shocks can at times exist [Feldman et al., 1984 and 1985; Smith et al., 1984]..

Feldman et al. [1984] first identified three plasmasheet/lobe crossings observed by ISEE-3 in the distant tail ($x < -200\ R_e$) which satisfied the Rankine-Hugoniot relations for nearly switch-offs] ow shocks. Traversing the shock from the upstream magnetotail lobe to the downstream plasmasheet, there was an abrupt decrease in magnetic field strength and an increase in the electron density and temperature. Feldman et al. [1984] also found a strong tailward-directed heat flux in the lobe. They pointed out that this feature is similar to those

which arc commonly observed at the earth's bow shock and are evidence for a magnetic connection across thelobe-plasmasheet boundary.

Smith et al. [1984] identified slow shocks using high resolution magnetic field data, They found that for some cases the shock normal had large inclination angles. The shock crossing times are about 30 sec. Assuming no tail motion, it implies that the shock has a thickness of about 10^3 km, a few times the ion inertial length - c/ω_{pi} (-700 km), where c is the speed of light and ω_{pi} is ion plasma frequency. The shocks are often associated with an enhanced level of hydromagnetic waves [Tsurutani et al., 1985] and plasma waves generated over a broad band of frequencies [Scarf et al., 1984].

Subsequently, Feldman et al. [1 985] used four criteria to examine the first distant tail passage of ISEE-3 between January 18 and February 11, 1983. They found a total of 26 slow-mode shocks. Using a 25 minute delay time, Feldman et al. examined the relationship between the slow shocks and near-earth substorm activity. They found that shocks were observed during all phases of substorm activity as well as during quiet times. They suggest that slow-mode shocks must therefore be a semipermanent feature of the bounding surfaces which separate lobe and plasmasheet in the distant geomagnetic tail, Recently Ho et al. [1 994] have shown a case of distant tail reconnection at x= -230 R_e. They see a near-complete reconnection signature which includes magnetic field B_z reversal (x neutral line), hi-directional plasma jetting and a pair of slow shocks.

Another interesting topic related to slow-mode shocks is the search for large rotational wavetrains downstream from such shocks. There have been more theoretical and simulation studies than observational studies on this topic. Based on two-fluid hydromagnetic theory, Coroniti [1971] first predicted the presence of large amplitude rotational wavetrains in the magnetic field downstream of a slow shock. In this theory, the damping of this dispersive wavetrain provides the necessary dissipation for the slow shock. However, this important feature has not yet been observed [Coroniti et al,, 1988]. . The absence of a wavetrain may suggest a dissipation mechanism different from that originally expected.

Many simulation studies have been conducted to explain this important difference between the observations and the theoretical predictions. Omidi and Winske [1989] showed that slow shocks have a wavetrain only when the upstream speed is subsonic and the ratio of electron to ion temperature is large enough to avoid Landau damping. Lee et al.[1989]

suggested the presence of a critical Mach number above which slow shocks have a wavetrain, and below which no wavetrain exists. A recent study by Omidi and Winske [1992] showed that the presence of wavetrains depends on the properties of upstream generated waves rather than the sonic Mach number or the ratio of electron to ion temperature as previously suggested.

A comprehensive survey of slow-mode shocks and their associated waves has not yet been conducted in the distant geomagnetic tail. Results of previous studies (see Feldman et al., 1985, and references therein) need to be extended to include the second distant tail pass of ISEE-3 with special attention given to the structures of slow-mode shocks, the relationships between slow-mode shocks and near-earth substorms, and the existence of downstream wavetrains. In the next section, we will first introduce the identification criteria of slow-mode shocks used in this study, These criteria emphasize use of magnetic geometry relations for all discontinuities in the lobe-plasmasheet boundaries as used in previous studies [Feldman et al., 1984 and 1985]. We have developed a five-step identification criterion for this purpose. In the third section we present all resultant parameters in statistical form. Included are the angles between the magnetic field and shock normal θ_{Bn}, Mach number, electron β_e, and tangential plasma flow velocity. We also show the distributions of shock thicknesses, and shock normal orientations. We present the correlation between near-earth substorm activity and the occurrence of slow-mode shocks, plasmoids and plasnlasheet/lobe crossings in the distant geomagnetic tail. We also report the results of a search for large amplitude wavetrains. Although such wavetrains are not found, some circularly polarized waves in the shock ramp regions are found instead. In section 6 we will discuss a possible model of steady reconnection in the distant tail which is responsible for the observed slow shocks, All results arc summarized in the last section.

2. Slow Shock Criteria

ISEE-3 made two distant tail swingby passes, the first between January 17 and February 15, 1983 at about x = -210 R_e and the second between June 23 to July 22, 1983 at about x = -230 R_e. Figure 1 shows the trajectories of both passes projected into the GSE equatorial plane. We have adopted criteria used by Bame et al. [1983] and Zwickl et al.[1984] to identify the various distant tail regions, such as the magnetosheath, mantle, lobe, plasmasheet boundary layer and plasmasheet. The magnetometer onboard makes three component observations with six readings per second (high resolution). The electron velocity is measured in two dimensions (V_x, V_y) with time separations ranging between 12

and 84 sec. An eight-hour time series of the magnetic field and electron measurements is shown in Figure 2 in GSE coordinate system (x is sunward, y is duskward and z is northward). The Figure clearly shows two plasmasheet/boundary crossings, which later are identified as slow-mode shocks. In the tail lobe, the magnetic field is stronger, with a large B_x component, and both the electron density and temperature are relatively low. Also, the plasma bulk velocity in the lobe is lower than that in the plasmasheet. Large-amplitude, low frequency waves are also seen near to but upstream of the slow-mode shocks, All boundary crossings from lobe to plasmasheet, or from plasmasheet to lobe, are counted individually as long as their time separation is greater than 10 minutes. Plasmoids are also identified by detection of a significant hi-polar signature in the B_z component of the downstream plasmasheet.

A definition to discriminate slow-mode shocks anti discontinuities requires the determination of the significant normal components of the magnetic field and the plasma velocity relative to the lobe-plasmashcet boundary. We accomplish this task through use of the magnetic field data to accurately determine the magnetic geometry of the boundary layer. We have developed a five-step identification criterion of slow shocks for this study as follows:

(1). All crossings between the plasmasheet and geomagnetic tail lobe field are selected mainly based on characteristic changes in the magnetic field (B_x component). All crossings are candidates for identification as slow-mode shocks. These criteria have yielded a total of 439 lobe-plasmasheet boundary crossings during the two tail passes of ISEE-3. However, 292 of these crossings are discarded because they were either so brief that they were judged to be incomplete boundary crossings, or such large fluctuations characterized the upstream or downstream regions that stable. values could not be found. Thus only those plasmasheet boundary crossings which had relatively stable value.s for at least 5 minutes in both the upstream and downstream regions were included in our study. A subset containing samples which were identified as having no significant increase in electron density, temperature and velocity were also eliminated for further study. The remaining 147 plasmasheet boundary crossings had jump conditions which are qualitatively consistent with those expected for slow-mode shocks. Most of them are isolated and not multiple plasmasheet boundary crossing events.

(2). Shock normals were calculated using magnetic data alone in the second step. We used the coplanarity theorem for this purpose,

$$\vec{n} // (\vec{B}_u - \vec{B}_d) \times (\vec{B}_u \times \vec{B}_d) / \left| (\vec{B}_u - \vec{B}_d) \times (\vec{B}_u \times \vec{B}_d) \right| \qquad (1)$$

where subscript u means the upstream lobe value, while d is the downstream plasmasheet value. The shock normals determined from formula (1) have certain errors. These errors may be estimated from the standard deviations in both upstream and downstream magnetic field in a shock coplanar coordinate system (i, j, k). On average, there is a deviation of ± 0.3 nT in the normal magnetic field, which will cause a f2.50 error in the shock normal determination. Other factors such as the presence of field fluctuations and/or waves in the upstream and/or downstream magnetic field can also cause errors. Thus, the total error in the shock normal may be greater than $\pm$ 5°. From an examination of the resultant set of shock normals, 21 events were found to have normal directions not in the x-z plane. These do not conform to ordinary ideas of slow-mode shock geometry, and we have thus not studied them in this work. We will examine them at a later date.

(3). The magnitude of the magnetic field normal relative to the plasmasheet boundary layer (B_n) was determined next. In order to definitively exclude tangential discontinuities from our data base, we adopted a minimum magnitude acceptance criterion for B_n amounting to 0.5 nT. For most cases there are significant B normal components across the shocks. However, we found that 11 cases had a smaller B normal component (magnitude < 0.5 nT).

(4). The geometry of the magnetic field in the shock frame was examined next, Five additional cases yielded a downstream θ_{Bn} larger than the upstream θ_{Bn}. These cases were eliminated from further study because their geometries were not consistent with those of slow-mode shocks. At this time, we do not fully understand what these structures might be. It is possible that they could be slow shocks superposed on top of fast-mode waves.

(5). Finally, the upstream plasma normal velocities were calculated using the Rankine-Hugoniot conservation relations. 'I'hey arc

$$B_{nu} = B_{nd} \qquad (2)$$

$$N_u V_{nu} = N_d V_{nd} \qquad (3)$$

$$V_{nu} B_{tu} - V_{tu} B_{nu} = V_{nd} B_{td} - V_{td} B_{nd} \qquad (4)$$

$$\frac{B_{tu} B_{nu}}{4\pi} - N_u m_p V_{nu} V_{tu} = \frac{B_{td} B_{nd}}{4\pi} - N_d m_p V_{nd} V_{td} \qquad (5)$$

where the subscript t means tangential component relative to the shock normal and m_p is proton mass. All physical quantities in the above equations are measured in the boundary

(shock) frame except the plasma flow velocity. A combination of actuations (2) though (5) gives a deduced upstream plasma normal velocity

$$V_{nu} = \left[\frac{V_{Anu}^2 (B_{tu} - B_{td})}{B_{tu} - (N_u / N_d) B_{td}} \right]^{\frac{1}{2}} \qquad (6)$$

The error of V_{nu} is estimated to be about ± 10 km/s based on the field standard deviations. Normal components of upstream plasma speeds in the boundary frame were calculated for 110 candidates in our data base using equation (6) to check whether they satisfied the slow-modc shock condition.

$$V_{SL} < V_n \leq V_{An} \qquad (7)$$

Here V_{An} *is* the Alfven speed *VA* in the shock normal direction, that is

$$V_{An} = V_A \cos \theta_{Bn} \qquad (8)$$

and V_{SL} *is slow mode velocity*

$$V_{SL} = \sqrt{\frac{(V_A^2 + C_s^2) - \sqrt{(V_A^2 + C_s^2) - 4V_A^2 C_s^2 \cos\theta_{Bn}}}{2}} \qquad (9)$$

Where

$$V_A = \frac{B}{\sqrt{4\pi N m_p}} \qquad (10)$$

and

$$C_s = \sqrt{\gamma k_B (T_e + T_p) / m_p} \qquad (11)$$

where $\gamma = 5/3$ is the specific heat ratio anti k_B is the Boltzman constant. For a low β plasma in the upstream lobe, because $C_s << VA$, *wc* have $V_{SL} = C_s$ when $\theta_{Bn}=0$, and $V_{SL} = 0$ when $\theta_{Bn}= 90°$. Due to the lack of thermal ion data in the ISEE-3 data set, wc assume that ions in the upstream tail lobe have a temperature of 3.5x1 0^5 K(3O eV) [Mukai, private communication, 1994]. We also define an intermediate Mach number M_I (relative to the intermediate speed V_{An}) which should always have a value ≤ 1.

$$M_I = M_{An} = \frac{M_A}{\cos \theta_{Bn}} = \frac{V_n}{VA \cos \theta_{Bn}} = \frac{V_n}{V_{An}} \qquad (11)$$

As shown in formula (6), when the downstream tangential field component (B_{td}) is near zero, the upstream plasma flow speed is equal to the intermediate Alfven speed. The slow-mode shock has the maximum strength ($M_I = 1$). We refer it as a switch-off shock because of disappearing tangential fields. Comparison of the inferred resultant velocities with both the lower 1 i mit (slow mode speed) and the upper limit (intermediate speed) in the upstream region, we find that 24 cases have speeds less than V_{SL} and so cannot be slow-mode shock. The remaining 86 crossings are slow-mode shocks and constitute the data base for statistical study reported next.

3. Statistical Results

A variety of plasma and field parameters that characterize the 86 individual slow-mode shocks that satisfied the acceptance criteria detailed in section 2 were cataloged and subjected to statistical analyses, This database has covered a broader range of the shock parameters, Using this dataset we may perform statistical studies to find the average properties and the distribution of slow-mode shocks. The results of this analysis are presented next.

Across all 86 slow shocks from the upstream lobe to the downstream plasmasheet, on average, we find that the magnetic field strength decreases from 10 nT to 3.7 nT, the electron density increases from 0.18 cm^{-3} to 0.31 cm^{-3}, the electron temperature increases from 7.6×10^5 K to 13.3x1 0^5 K, and the measured plasma flow velocity also significantly increases from 170 km/s to 652 km/s. The dependence of slow shock structures on a variety of plasma and field parameters will be studied first. These include a) the angle θ_{Bn} between the magnetic field and the shock normals, b) both upstream and downstream Alfven Mach number M_{An} (or M_I), c) electron plasma β_e, d) downstream tangential flow speeds, V_x, and e) the shock thickness.

The θ_{Bn} angles of the shock are key parameters in determining the shock structure. The orientations of magnetic fields relative to the shock normal play an important role in controlling the particle reflection and wave. propagation. Figures 3a and 3b show the shock distributions of both upstream and downstream θ_{Bn}. We see from Figure 3a that the upstream angles are mainly distributed between 65° and 85°, with an average of 74°. l'here are 9 cases with $\theta_{Bn} > 85°$. When considering a larger error, some of them may be out of this range. Downstream θ_{Bn} angles have a broader distribution, with an average of 50°. Note that the downstream magnetic field B_d is always greater than B_n, indicating that pure switch-off shocks are not found. However, three events have very small downstream θ_{Bn} angles below 15° and therefore they approach the switch-off shock condition. Their upstream θ_{Bn} angles are 45°, 64° and 70°, respectively, In contrast, there are 14 slow shocks with large downstream θ_{Bn} greater than 70°. These slow shocks are mainly detected in the crossings between the lobe and the plasmasheet boundary layer.

The upstream Mach number and plasma beta are two other important parameters for the shock. The slow shock dependence on upstream intermediate Mach number M_I and electron β_e are shown in Figure 4a and 4b. The intermediate Mach number may reflect the

strength of the slow shock. From equation (11), when $M_I = 1$, that is, the inferred $V_{un} = V_{An}$, the shock has the maximum intensity. From Figure 4a we see that M_I has a distribution above 0.6 with an average of 0.87 and a trend to one. There are21 cases with $M_I > 0.95$ and 5 cases with $M_I > 0.98$ which is close to the switch-off shock limit. As shown in Figure 4b, electron β_e in the upstream region is very low, since in the tail lobe, there are strong magnetic fields and low electron densities and temperatures. The electron β_e is mainly distributed below 0.1 with an average of 0.04. The downstream plasmasheet has a high plasma beta, increasing at least by a factor of 30. Thus, we expect larger Landau damping there for low frequency waves.

Occurrence rates as functions of the shock thickness and the measured downstream tangential plasma flow speed V_x *are* shown in Figure 5a and 5b. Because the shock speed relative to the spacecraft is unknown, it is difficult to determine the thickness of a slow shock. Feldman et al. [1987] used the cross-shock currents to calculate the thickness of the slow-mode shock from ISEE-2 observations. Because ISEE-3 did not have ion measurements in the distant tail, a similar determination for the present data set is not possible. However, because our study is based on a large dataset, wc will estimate shock thicknesses from measured boundary layer transit times, under the assumption that the shocks have an average speed of 20 km/s relative to the. spacecraft [Scarf et al., 1984; Smith et al., 1984]. The resultant distribution is shown in Figure 5a. Inspection reveals a very broad distribution of thicknesses up to 14,000 km, with an average of 5380 km (about 7 ion inertial lengths). There are 12 shocks with thicknesses greater than 10,000 km.

From Figure 5b we see that downstream plasmasheet plasma flows are mainly in the tailward (-x) direction, averaging -585 km/s. This speed is higher than the average flow speed (-5 15 km/s) associated with those non-shock plasmasheet boundary crossings. In contrast, downstream plasmasheet flows in the y direction are much lower, averaging around 20 km/s but with large fluctuations ranging from -180 to 200 km/s. We have found that two of the 62 slow shock cases in our data base have earthward flows. Assuming that these earth ward flows are from the reconnect on region (of the Petcheck model), they arc then definitely from the earthward side of the distant neutral line,

Figure 6 shows one of two cases in plasma and magnetic field data. We see that the spacecraft enters the plasmasheet from the north lobe across a slow shock at 09:16 UT and immediately detects a significant earthward flow ($+V_x$ -300 km/s). At about 10:00 UT the spacecraft enters the south lobe and we note a reduced plasma velocity. Then in the next

two hours the spacecraft returns to the plasmasheet and traverses from a position earthward to tailward (or vice versa) of the neutral line. This indicates that the neutral line may exist beyond 217 R_e in the distant tail. At 12:30 UT the spacecraft is completely out of the plasmasheet and into the south lobe. When we examine the near-earth magnetic activity index (AE) during the same interval, we see that the magnetic activity is quiet before 11:30 UT. The second slow shock case of the neutral line encounter associated with hi-directional plasma jetting flows in the distant tail has been reported in a recent study [Ho et al., 1994].

Distributions of the shock normals in two orthogonal planes (x-z and y-z) are shown in Figures 7a and 7b. On average, the angle between the shock normals and the z axis, $\theta_{zn} = cos^{-1}n_z$ = 22,4°. Note that the projection of the normals in the x-z plane are smaller than those in the y-z plane. This result is consistent with a plasmasheet boundary layer that is closely along the x direction. This suggests that the slow shock surface is twisted around the x-axis due to IMF BY. We further note that the average inclination angle between the shock normal in the x-z plane and z axis is 13.8° and that in the y-z plane is 15.2°. These orientations are consistent with the cartoon presented in Feldman et al. [1985], of two slowly flowing surfaces that bound a relatively thin, extended plasmasheet. It is less accurate to deduce the neutral line location by using the tilt angle of the slow shock normal from single events, because the tail flapping may significantly change the shock orientations. However, wc can estimate the distance of the neutral line to the spacecraft using an average shock tilt angle in the x-z plane. Based on the tilt angle, wc find that the neutral lines are located in the range from -160 to -240 R_e (200±40 R_e).

4. Correlation with Substorms

According to the simple model of tail magnetic reconnection in the geomagnetic tail proposed by Petschek [1 964], slow-mode shocks provide an important means for converting the magnetic energy in the lobes into the plasma kinetic or thermal energ y in the plasmasheet. However, the connection between this process and the well known effect of substorms in the inner magnetosphere has not yet been established, For example, the slow-mode shocks in the deep tail may be associated with the passage of transient plasmoids formed in the recovery phases of substorms, or they may be a semipermanent phenomenon which stands in the boundary surface. In addition, near-earth substorm activity occurs so frequently that inter-storm quiet times are often absent. It is therefore difficult to obtain one-to-one identification of isolated substorms and distant tail events. Thus, in the present study, we have taken a different approach to determine correlation with substorms.

Our assumption is that if there is a connection between the near-earth substorms and distant tail dynamics, strong geomagnetic activity (high AE indices) should be associated with high occurrence rates of slow shocks and plasmoids in the distant tail. An appropriate time delay must be used to account for the finite plasma propagation speed. In order to test this conjecture, we extend the statistics into a 60 day time period to fully cover the two ISEE-3 tail passes. The statistics have been performed separately for both conditions: southward IMFs and northward IMFs. We have used 10 minute averages of the IMF (from IMP-8) and the AE index for this study. The data distribution is shown in Figure 8. As expected, northward IMFs arc associated with low AE indices, while southward IMFs show a correlation with AE values. We have assume.d a 40 minute lag corresponding to a plasma flow speed of 530 km/s from the near earth. All the slow-mode shocks, plasmoids and plasmasheet boundary crossings are identified to be present or not in each 10 minute interval. The plasmoids and plasmasheet/lobe crossings are identified using the definitions stated before. A plasmoid may be associated with a slow shock or a non-shock crossing. Their occurrence rates are normal ized by the time intervals.

in order to determine the relationship of IMF orientations to the distant tail events, we examine the data when the IMF B_z >2 nT anti B_z <-2 nT because substorms will probably not be triggered during those intervals with small field fluctuations. We have found that of 28 available slow shocks, 15 occur during a southward JMF(18% interval) and 13 appear in a northward IMF (21 ‰ interval). The occurrence dependences of all slow shocks, plasmoids, and plasmasheet/lobe crossings on the AE index are shown in Figures 9a (southward IMFs) and 9b (northward IMFs). The error bars are also given based on data coverage. From Figures 9a we note some AE dependence for the occurrence rates of slow-mode shocks, plasmoids and plasmasheet boundary crossings. Three occurrence rates reach their maximum between 300 and 600 nT in AE index. This indicates that during strong southward IMFs, the distant tail events indeed have some relations with near-earth substorm activities. However, from Figure 9b we do not find such AE dependence for all occurrence rates. We find that slow shocks and plasmoids also occur during northward IMFs and low AE intervals. This may indicate that they have the different generation mechanism from those during southward IMF intervals, We have also tested this dependence using other lag times (20, 30 and 50 min.) between the AE index and distant tail observations and B_z restrictions. The weak substorm dependence does not change with different lag times and with all IMFs. Our results are in general consistent with the earlier study of Feldman et al. [1985], that slow-mode shocks in the distant geomagnetic tail may

be independent of near-earth substorm activity. We note that the occurrence rate of plasmasheet crossings peak between the 400 and 600 AE. This may indicate that the distant tail becomes more dynamic during the magnetic active times.

In a reconnection process, a plasmoid (plasma jetting accompanied by a bipolar B_z signature) is expected to be associated with the formation of a magnetic field neutral line and slow-mode shocks. The study of Hones et al. [1984] shows that plasmoids in the distant tail are strongly correlated with substorms, but have a 20-30 minute lag between substorm onsets and plasmoid detection at ISEE-3. Moldwin and Hughes [1993] also examined all plasmoids encountered by ISEE-3 in the distant tail. They found that over 84% of 366 plasmoid events occurred between 5 and 60 minutes after a substorm onset. However, the plasmoid occurrence maximizes at moderate K_p levels (- 3), instead of larger K_p values. We have taken a statistical approach and have found a different results in agreement with those of much more previous studies. Tsurutani et al. [1987] show that the large scale field variations with North-then-South signatures across the plasmasheet boundaries occur during all geomagnetic activity levels in the distant tail. In addition, during magnetic quiet times, plasmoid propagating tailward from 100 R_e [Scholer et al., 1986], and occasional earthward propagating plasmoids in the mid-tail region (-90 R_e) [Siscoe et al., 1984] have been reported. In a recent study, Saito et al. [1 995] have examined the geomagnetic activity dependence of GEOTAIL observations. They find that all boundary crossings increase with increasing K_p index up to K_p=5. But the occurrence rate of slow-mode shocks does not show a clear dependence on K_p index. All of these features show that the distant tail phenomena arc not simply related to near-earth magnetic activity. Some steady distant reconnection processes which are independent of near-earth magnetic activity may play certain roles in generating these plasmoids and slow shocks. We have proposed a model to explain the slow shocks and plasmoids detected in the deep tail during northward IMF periods [110 and Tsurutani, 1995].

5. Search for slow shock wavetrains

Previous studies of the structure of slow-mode shocks in the distant geomagnetic tail have not found trailing cyclotron wavetrains as predicted by Coroniti [1971]. This result has stimulated further work in computer shock simulations. We in turn have searched our expanded data base for evidence of large wavetrains associated with 86 slow-mode shock events identified during both ISEE-3 tail passes.

According to theory, large amplitude cyclotron wavetrains should appear within the trailing edge, downstream of slow-mode shocks. Because they have a left-handed circular polarization, when z is along the shock normal direction, the wavetrains should mainly appear as correlated variations in B_x and B_y, having a 90° phase difference. They should also have amplitudes similar in magnitude to the upstream magnetic field intensity. The numerical simulations predict the largest amplitudes for the strongest slow-mode shocks, i.e., switch-off shocks. They should also have a wavelength of about several ion inertial lengths, which should be comparable to the thicknesses of the shocks. Although significant fluctuations in B and multiple crossings of the lobe-plasmasheet boundary arc often encountered in the deep geomagnetic tail, a close evaluation of all 86 definite shocks cataloged in the present study has failed to reveal the rotational wavetrains as predicted.

One possibility is that downstream wavetrains arc damped. A recent simulation [Fujimoto and Nakamura, 1994] shows that the presence of heavier O+ ions may strongly damp these downstream wavetrains. In a more recent kinetic simulation, Omidi and Winskc [1992] also show that damping is not the only way in which the wavetrains can be eliminated. Other effects, such as a nonsteady shock behavior, can also have a similar effect. They found that there are four general types of shock structures in which lithe or no wave activity may be present both upstream and downstream of the shock. Our present observations cannot distinguish among these possibilities.

Even though we did not find large amplitude wavetrains downstream of slow-mode shocks, medium amplitude waves sometimes are noted in the upstream ramp regions. Figure 10 shows one example on January 28, 1983. We see that around 23:55 UT the magnetic field has a slow shock transition from the plasmasheet to the south lobe. In the middle of the shock ramp, there is moderate wave activity in the y and z components associated with a significant dawnward plasma flow. The waves last about 50 see, compared with a 90 sec duration of the slow shock gradient, The changes of the background field mainly take place in the B_x component, while average B_y and B_z have very small variations across the shock. However, in the B_x component and total magnetic field strength no obvious wave activity appears in the shock ramp. Thus these shock ramp waves are primarily transverse waves. They have peak to peak amplitudes of 3 nT and a $\Delta B/B$ ratio of 0.28. The waves in this case have periods between 10 and 20 sec or frequencies from 0.05 to 0.1 Hz near the ion cyclotron frequency. Polarization analyses shows that they are right-hand circularly polarized.

Note the presence of large amplitude waves in the upstream region around 00:15 UT. These are well-defined, right-hand circularly polarized waves. They were first reported by Tsurutani and Smith [1984] and were identified as the ion cyclotron waves in the plasmasheet boundary layer [Tsurutani et al., 1985], All features which wc found for the shock ramp waves are the same as these waves appearing in the plasmasheet boundary layer. Scarf et al. [1984] have found intense broadband electrostatic noise or lower hybrid waves appearing in the shock layer. Coroniti et al. [1994] have shown two examples of the Alfven/ion cyclotron waves in the slow shock ramp regions. However, these medium amplitude magnetic waves peaking in the gradients of the shocks are reported for the first time in detail.

Six cases with obvious shock ramp waves are found in the 86 slow shock events. Almost all of these shocks have large upstream θ_{Bn} (> 800), very small θ_{zn} (< 150), large shock thickness (> 4000 km) and high *Ml* (*> 0.90). The* waves generally peak in the middle of the shock gradients. It seems that there is no direct connection between these waves and the boundary layer waves far upstream of the shocks. But we can always sec some small amplitude waves appearing between them. These shock ramp waves may provide resistivity for energy dissipation.

6. Discussion

From slow-mode shock parameter analyses, slow-mode shock parameters cover a relatively small range, compared with the earth's bow shock. For a slow shock in the distant tail, because the upstream field mainly is in the x direction, wc see a larger θ_{Bn} angle distribution for the upstream field. They are mainly quasi -perpendicular shocks, because all upstream θ_{Bn} angles are >45°.

Compared with the previous studies, our database includes 23 of the 26 slow shocks identified by Feldman et al. [1 985] and Schwartz et al. [1 987] during the first ISEE-3 distant tail pass. The remaining three plasmasheet boundary crossings are so transient and the upstream magnetic field is fluctuating so rapidly that it is difficult to apply coplanarity theory to them. They therefore failed to pass our first criterion. Feldman et al. [1985] found that the slow shocks identified in their study were relatively strong. The Alfven Mach numbers were an average of 0.94 in the range from 0,9 to 0.98. This range lies close to the switch-off limit. In addition, the average density compression ratio (n_d/n_u) in their shock set was 2.5. Our data base shows that slow shocks have a large range of Mach numbers, from

0.56 to 0.99, and average densities jump by a factor of 1.7, in the range from 1.1 to 7.5. The thickness of slow shocks is much larger than that of the earth's bow shock which usually has short ion initial length, Theoretical study predicted that a slow shock would have large thicknesses [Coroniti, 1971]. Our observation results are consistent with this prediction.

Our results further confirm the existence of the distant reconnection. However, there are some differences between our observations and previous models [Richardson et al., 1989]. First, previous observations indicate that the distant tail neutral line is located at about -120 R_e, because beyond this distance the plasma flows in the plasmasheet are dominantly in tailward [Zwickl et al., 1984], Our statistical study based on slow-mode shocks shows that the distant neutral lines may be extended at least to 200 R_e. This is generally consistent in the deep tail reconnection, rather than the near-earth reconnection. We think that experimental errors and variations in reconnection location can cause these discrepancies.

Second, we find a weak substorm dependence for the distant tail slow-mode shock occurrence. This is an average results for both magnetic disturbed (southward IMFs) and quiet times (northward IMFs). We indeed note that many slow-mode shock events in the distant tail have very good correlation with near-earth substorms and large AE indices, These events often correspond to large tail ward plasma flows (- 1000 km/s) and negative B_z in the downstream plasmasheet. They may be related to downtail plasma flows accelerated by the near-earth reconnection during substorms. However, for near half of distant tail slow-mode shock cases, they occur during northward IMF or low AE periods. We have proposed a northward IMF distant neutral line model to explain these observed slow shocks [Ho and Tsurutani, 1995]. During northward IMF intervals, the IMF lines may penetrate the tail through a reconnection in the cusp region. Then these field lines are bent and kinked inside the plasmasheet to form the distant neutral line. Using this model and the standard substorm reconnection model during southward IMFs [Richardson et al., 1989], we may explain almost all distant tail observations .

Initial theoretical studies predicted that large amplitude Alfven rotations of the magnetic field should provide the required resistance for shock dissipation. However, recent kinetic simulation studies show that under certain conditions the shocks may exhibit no waves. We have examined some cases of the existence of upstream ion cyclotron waves and shock ramp waves. Due to the absence of ion data, wc cannot exactly compare these observations

with the simulations. A further analysis of wave properties to classify all the shocks into different categories of θ_{Bn} angles and Mach numbers is still needed.

7. Summary

We have performed the first detailed study examining all of the ISEE-3 distant tail (> 200 R_e) data to examine every plasrnashect/lobe crossings and to identify slow-mode shocks. We also have searched for large amplitude circularly polarized waves predicted by simulation/theory. Substorm dependence on the existence of shocks/nonshocks are examined statistically. From 60 days of data spanning two distant tail passes, we find 439 plasmashect/lobe crossings. Among these crossings, 77 events are associated with plasmoids and 86 events are identified as clear slow shocks. Therefore, 377 plasmasheet crossings can not be defined as slow-mode shocks, because they do not satisfy our criterion. While 33 plasmoids are accompanied by slow shocks, the other 51 plasmoids simply occur with plasmasheet crossings. Through a statistical study based on GEOTAIL observations, Saito et al. [1995] also find 32 confirmed slow-mode shocks from 303 plasmasheet crossings. Their ratio (1 1%) is lower than that (19%) wc found based on ISEE-3 observations.

in our study, we find no pure switch-off shocks with downstream θ_{Bn}= O. However, many cases show large Mach numbers nearly at the switch-off limit. The slow shocks have relatively large thicknesses which may reflect large cyclotron radius downstream of the shocks. We see a dominantly tailward plasma flow in the plasmasheet of the distant tail. Only two of the 62 shocks had a downstream earthward flow. We find essentially a weak correlation between the near earth AE index and the occurrence of distant tail slow-mode shocks, in agreement with previous findings. Although the slow-mode shock is not a permanent feature as a boundary surface separating the plasmasheet from the tail lobes, it is a significant feature of the structure of the distant geomagnetic tail. A statistical summary of many plasma parameters delineating the structure of these shocks has yielded many significant results as following.

1. Using five criteria based on magnetic field geometry and plasma conditions, from 439 plasmasheet/lobe crossing in the distant tail, we have found definite 86 slow-mode shocks which all satisfy the Rankine-Hugoniot relation and the slow-mode shock condition ($V_{SL} < V_n \leq V_{An}$). We also detect 77 plasmoid events associated with the plasmasheet crossings. Among these events, 33 plasmoids are found to be associated with slow shocks.

2. Across the slow shocks from the upstream to downstream regions, the magnetic field, on average, decreases by a factor -2.7 in the range from 1.4 to 9,0; electron density increases by ~1.7 with a range from 1.1 to 7.5 and temperature increases by ~1.8 with a range from 1.1 to 3.5, while plasma flow velocity increases on average by a factor of -3.8 and ranges between 2 and 14. Based on the coplanarity theorem, we have found that there is a large average upstream θ_{Bn} angle of 70° and a small downstream θ_{Bn} angle of 50°. The shocks have an average intermediate Mach number of 0.87 and an upstream β_e of 0.04.

3. In the downstream, the plasma flow associated with the shocks is dominantly in the tailward direction with an average of 585 km/s. The shock thickness is estimated roughly around 5000 km on average (about 7 ion inertia lengths). The shocks have an average θ_{zn} of 22.4° between the shock normal and z axis. In the x-z plane, this tilt angle relative to the z axis is 13.8°. Using Petschek's simple slow shock model and the orientation of these slow shocks, we deduce that the neutral lines are in the range from -160 to -240 R_e in the distant tail.

4. During the southward IMF intervals with B_z <-2 nT, the occurrence rates of slow shocks and plasmoids in the distant tail have a dependence on near-earth substorm activity. This suggests that tailward traveling plasmoids from the near-earth are responsible to these distant tail events. However, no such dependence is found during northward IMF periods. Nearly half of slow-mode shock events occur during the northward IMF intervals. The plasmasheet/lobe crossings are more frequent during substorm times, indicating that the distant tail becomes more dynamic.

5. We do not find any large rotational wavetrains in the downstream slow shocks as expected by MHD theory/numerical simulations. This result does not seem to depend on Mach number and θ_{Bn} angles. Instead, we do see some (6 cases) medium amplitude waves appearing in the ramp regions of slow shocks which usually have large M_I and upstream θ_{Bn}. These waves are similar to the right-hand ion cyclotron waves appearing in the plasmasheet boundary layer.

Acknowledgments: The research conducted at the Jet Propulsion Laboratory, California Institute of Technology was performed under contract to the National Aeronautics and Space Administration.

References

Bame, S. J., R. C. Anderson, J. R. Asbridge, D.N.Baker, W. C. Feldman, J.T.Gosling, E. W. Hones,Jr., D. J. McComas, and R.D.Zwickl, Plasma regimes in the deep geomagnetic tail: ISEE-3, Geophys. Res. Lett., 10, 912, 1983.

Coroniti, F. V., Laminar wave-train structure of collisionless magnetic slow shocks, Nuclear Fusion, 11, 261, 1971,

Coroniti, F. V., F. L. Scarf, and C.F.Kennel, A search for lower hybrid drift turbulence in slow shocks, J. Geophys. Res., 93, 2553, 1988.

Coroniti, F. V., S. L. Moses, E. W. reenstadt, B. T. Tsurutani, and E. J. Smith, Magnetic and electric field waves in slow shocks of the distant geomagnetic tail: ISEE 3 observations, J. Geophys. Res., 99, 11251, 1994.

Feldman, W. C., S. J. Schwartz, S. J. Bame, D. N. Baker, J. Birn, J. T. Gosling, E. W. Hones, Jr., D. J. McComas, J. A. Slavin, E. J. Smith, and R. D. Zwickl, Evidence for slow-mode shocks in the distant geomagnetic tail, Geophys. Res. Lett., 11, 599, 1984.

Feldman, W. C., D. N. Baker, S. J. Bame, J. Birn, J. T. Gosling, E. W. Hones, Jr., S. J. Schwartz, and R. D. Zwickl, Slow-mode shocks: A semipermanent feature of the distant geomagnetic tail, J. Geophys. Res., 90, 233, 1985.

Feldman, W. C., R. L. Tokar, J. Birn, E. W. Hones, Jr., S. J. Bame, and C. T. Russell, Structure of a slow-mode shock observed in the plasmasheet boundary layer, J. Geophys. Res., 92, 83, 1987.

Fujimoto, M. and M. Nakamura, Acceleration of heavy ions in the magnetotail reconnection layer, Geophys. Res. Lett., 21, 2955, 1994.

Ho, C. M. and B. T. Tsurutani, Distant tail plasma jetting and Bz properties at slow-mode shocks: A model of reconnection during northward IMF, Geophys. Res. Lett., 1995, in press.

Ho, C, M., 13, T. Tsurutani, E. J. Smith, and W. C. Feldman, A detailed examination of a X-line region in the distant tail: ISEE-3 observations of jet flow and Bz reversals and a pair of slow shocks, Geophys. Res. Lett., 21, 3031, 1994.

Hones, E. W., Jr., J. R. Asbridge, S. J. Bame, W. C. Feldman, J. T. Gosling, D. J. McComas, R, D. Zwickl, J. Slavin, E. J. Smith, and B. T, Tsurutani, Structure of the magnetotail at 220 R_E and its response to geomagnetic activity, Geophys. Res. Lett., 11,5, 1984.

Kennel, C. F, J. P. Edmiston, and T. Hada, A quarter century of collisionless shock research, in *Collisionless Shocks in the Heliosphere: A Tutorial Review, Geophys.*

Monogr. Ser., vol.34. p. 1, edited by R. G. Stone and 13. T. Tsurutani, AGU, Washington D. C., 1985.

Lee, L.. C., Y. Lin, Y.Shi, and B. T, Tsurutani, Slow shock characteristics as a function of distance from the X-line in the magnetotail, Geophys. Res. Lett., 16,903, 1989.

Moldwin, M. B., and W.J. Hughes, Geomagnetic substorm association of plasmoids, J. Geophys. Res., 98, 81, 1993.

Omidi, N., and D. Winske, Structure of slow magnetosonic shocks in low beta plasma, Geophys. Res. Lett., 16, 907, 1989.

Omidi, N., and D. Winske, Kinetic structure of slow shocks: Effects of the electromagnetic ion/ion cyclotron instability, J. Geophys. Res., 97, 14801, 1992.

Petschek, H.E., in *Magnetic field annihilation, AAS-NASA symposium on the physics of solar flares, edted by W. N. Hess,* NASA SP-50, P425, 1964.

Richardson, and S. W. H. Cowled, Plasmoid-associated energetic ion burst in the deep geomagnetic tail: Properties of the boundary layer, J. Geophys. Res., 90, 121 ?J3-12158, 1985.

Richardson, I. G., C. J. Owen, S. W.H.Cowley, A. B. Galvin, T. R. Sanderson, M. Scholer, J. A. Slavin, and R. D. Zwickl. ISEE-3 observations during the CDAW 8 intervals: Case studies of the distant geomagnetic tail covering a wide range of geomagnetic activity, J. Geophys. Res., 94, 15189, 1989.

Saito, Y ., T. Mukai, T. Terasawa, A. Nishida, S. Machida, M. Hirahara, K. Maezawa, S. Kokubun, and T. Yamamoto, Slow-mode shock in the magnetotail, J. Geophys. Res., 1995, in press,

Scarf, F.].., F. V. Coroniti, C.F.Kennel, E. J. Smith, J. A. Slavin, B. T. Tsurutani, S.J. Bame, and W.C. Feldman, Plasma wave spectra near slow-mode shocks in distant magnetotail, Geophys. Res. Lett., 11, 1050, 1984.

Scholer, M., G. Gloeckler, B. Klecker, F. M.Ipavich, D. Hovestadt, and E. J. Smith, Fast moving plasma structures in the distant magnetotail, J. Geophys. Res., 89, 6717, 1984.

Schwartz, S. T., M. F. Thomsen, W. C. Feldman, and F. T. Douglas, Electron dynamic and potential jump across slow-mode shocks, J. Geophys. Res., 92, 3165, 1987.

Siscoe, G. L., D. G. Sibeck, J.A. Slavin, E.J.Smith, B. T. Tsurutani, and D.E.Jones, ISEE-3 magnetic field observations in the magnetotail: implications for reconnection, in *Magnetic Reconnection in Space and Laboratory Plasma, Geophys. Monogr. Ser., vol.30.* p. 240, edited by E.W.Hones, AGU, Washington D. C., 1984.

Smith, E. J., J. A. Slavin, B. T. Tsurutani, W,C.Feldman, and S. J.Bame, Slow-mode shocks in the earth's magnetotail: ISEE-3, Geophys. Res. Lett., 11, 1054, 1984.

Sonnerup, B.U.O., Magnetic re-connection in a high] y conducting incompressible fluid, J. Plasma Phys., 4, 161, 1970.

Tsurutani, B. T., and E. J. Smith, Magnetosonic waves adjacent to the plasma sheet in the distant magnetotail, Geophys. Res. Lett., 11, 331, 1984.

Tsurutani, B. T., I. G. Richardson, R.M.'1'horne, W. Butler, E.J.Smith, S. W. H. Cowled, S.P. Gary, S.-I. Akasofu, and R.D. Zwickl, Observations of the right-hand resonant ion beam instability in the distant plasmasheet boundary layer, J. Geophys. Res., 90, 12159, 1985.

Tsurutani, B. T., B. E.Goldstein, M. E. Burton and D. E.Jones, A review of the ISEE-3 geotail magnetic field results, Planet. Space Sci., 34, 931, 1986.

Tsurutani, B. T., M.E.Burton, E. J. Smith and D. E. Jones, Statistical properties of magnetic field fluctuations in the distant plasmasheet, Planet. Space Sci., 35,289, 1987.

Zwickl, R. D., D. N, Baker, S. J. Bame, W. C. Feldman, J.T.Gosling, E.W.Hones Jr., and D.J.McComas, Evolution of the Earth's distant magnetotail: ISEE-3 electron plasma results, J. Geophys. Res., 89, 11,007, 1984.

C. M. Ho, B. T. Tsurutani and E. J. Smith (Jet Propulsion Laboratory, California Institute of Technology, Pasadena, CA 91109; Tel. 818-354-7894).

w. C. Feldman (Los Alamos National Laboratory, Los Alamos, NM 87545)

Figure Captions

Figure 1. The two distant tail passes of ISEE-3. ISEE-3 had the aid of the moon's gravity to complete two distant tail passes at -210 R_e and -230 R_e respective] y. Trajectories are shown in the equatorial plane in GSE coordinates.

Figure 2. Two slow shock examples in an eight hour time series observed by ISEE-3 around x = -210R_e during its first distant tail pass on February 10, 1983. From top to bottom are electron density N_e, electron temperature T_e, electron plasma velocity (two components and total V), magnetic field (three components and total strength) in GSE coordinates. Two plasmasheet crossings are accompanied by significant increases in N_e, T_e and V, as well as a decrease in the magnetic field B. We also see strong low frequency wave activity associated with the slow shocks in the boundary layer, Top bar gives the locations in the distant tail (shaded, plasmasheet).

Figure 3. Distributions of the angles between the shock normal and the magnetic fields for (a) upstream and (b) downstream, Upstream θ_{Bn} angles peak at around 80°, while downstream θ_{Bn} angles have a broader distribution.

Figure 4. Distributions of (a) intermediate Mach number and (b) upstream electron β_e for all slow shocks. The Mach numbers in the normal M_I maximize around 0.9, while most shocks have smaller upstream β_e below 0.04.

Figure 5. The shock number dependence on (a) shock thickness and (b) on the downstream plasma speeds. The thickness of the shocks has a broader distribution up to 14,000 km. The dominant tailward plasma flows are greater than 400 km/s.

Figure 6. An example of the earthward plasma flow associated with slow shocks on January 29, 1983, From top to bottom in consequence are electron density, electron temperature, plasma bulk flow velocity (two components and total speed), and magnetic field data. Around 09:20 UT, crossing a slow shock, the spacecraft enters the plasmasheet on the earthward side of the neutral line. Then the plasmasheet goes up and down relative to the spacecraft. At about 12:30 UT it returns to the lobe. Top bar shows the locations in the distant tail (shaded, plasmasheet; SL, south lobe; NL, north lobe).

Figure 7. The distributions of the shock normal n in (a) x-z plane and (b) y-z plane. Note that the shock normal may have an uncertainty of 180°, The shock normals have larger tilt angles in the x-z plane than in the y-z plane relative to the z axis.

Figure 8, The relationship between upstream IMF B_z and AE index for the period of two ISEE-3 distant tail passes. IMF data are from IMP-8's observations inside solar wind. Both data have 10 min. time resolution. A 10 min delay of IMFs relative to AE is used for this plot. Near earth magnetic field becomes more active (large AE) with increasing negative IMF B_z. The average variation is also shown in the plot.

Figure 9. Occurrence rates of slow shocks, plasmoids and plasmasheet crossings as functions of the AE index (with each bin of 100), separately for southward IMFs a) and northward IMFs b) for IMF $|Bz| > 2$ nT intervals. There is a 40 min lag of AE values relative to the tail observations. 'l'he error bars arc also given for each line. While there are some substorm dependence for the occurrence. of slow-mode shocks and plasmoids during southward IMFs, there is no such dependence during northward IMF periods. There are peaks for plasmasheet crossings between 400 and 600 AE.

Figure 10. A slow shock and shock ramp waves at around 23:55 UT, January 28, 1983. Mid-amplitude waves appearing in the shock gradient regions are transverse waves. Plasma data show a large dawnward ($-v_y$) plasma flow around the same time. The waves appearing at around 00:15 UT with large amplitudes are boundary layer waves which are generated by the ion cyclotron resonant instability.

ISEE-3Distant Tail Passes

Pass 2

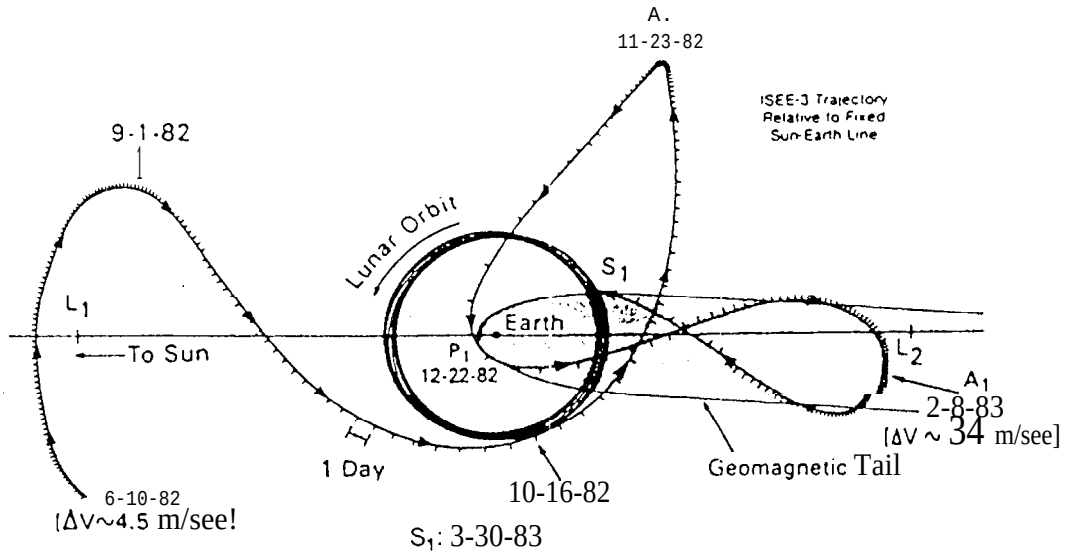

Pass 4

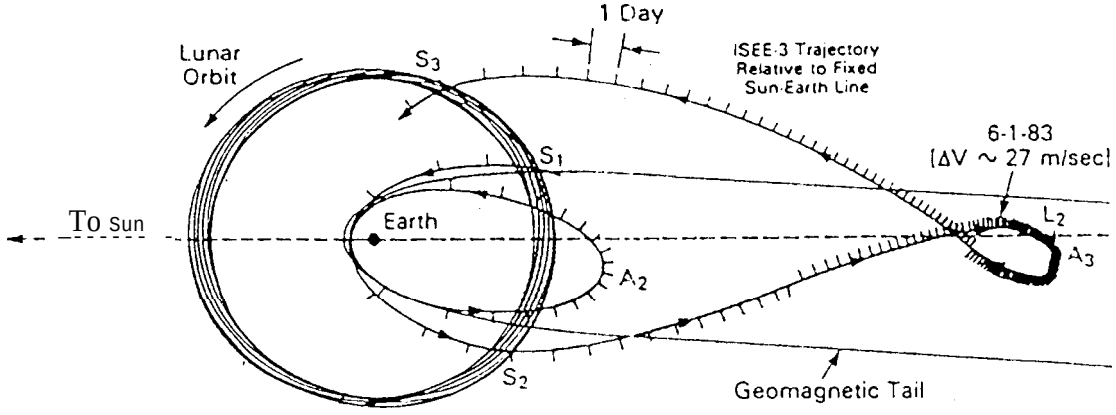

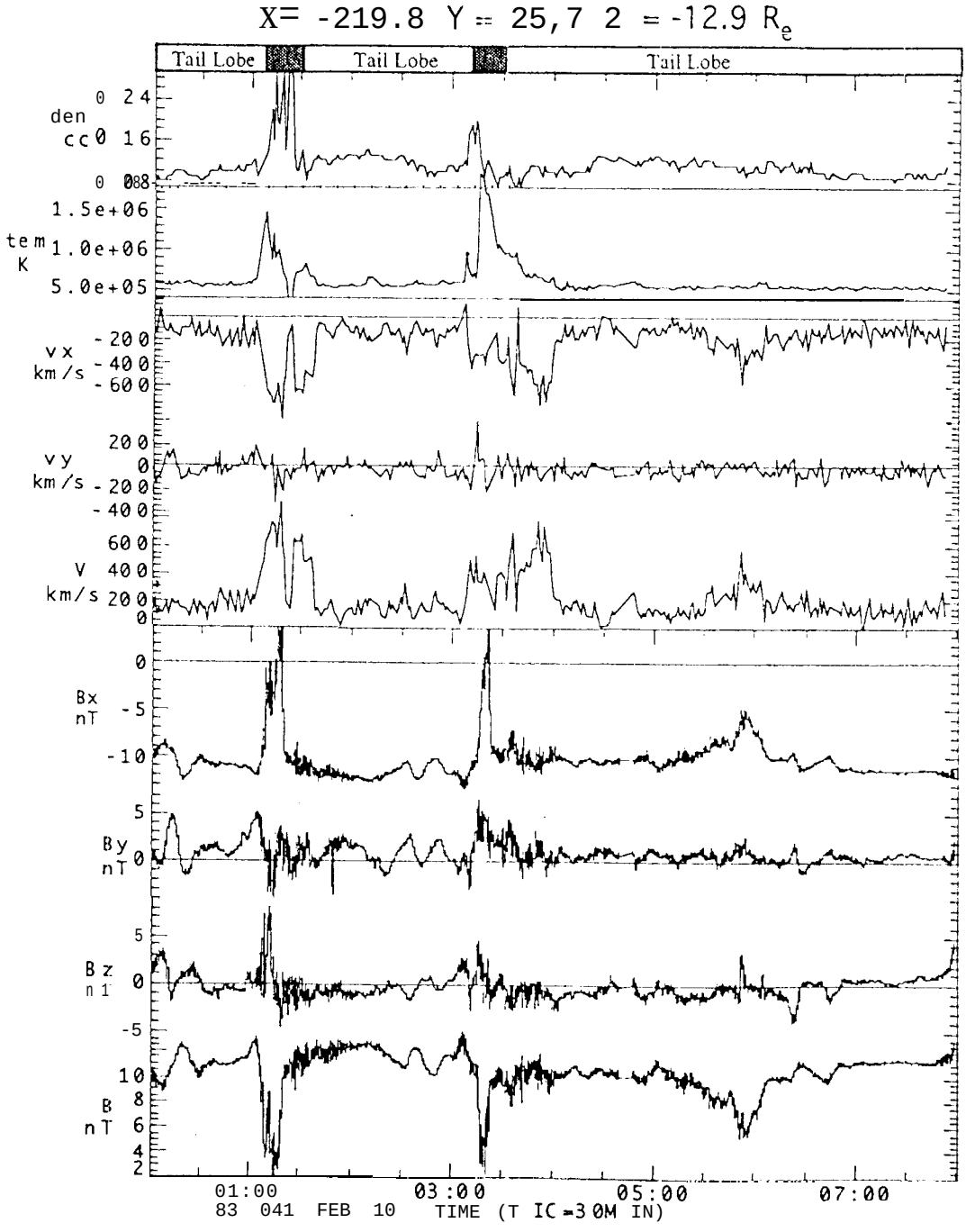
X= -219.8 Y = 25,7 2 = -12.9 Re
Tail Lobe
Tail Lobe
Tail Lobe
den cc
0 24
0 16
0 088
tem K
1.5e+06
1.0e+06
5.0e+05
vx km/s
-200
-400
-600
vy km/s
200
0
-200
-400
V km/s
600
400
200
0
Bx nT
0
-5
-10
By nT
5
0
Bz nT
5
0
-5
B nT
10
8
6
4
2
01:00
03:00
05:00
07:00
83 041 FEB 10 TIME (T IC=30M IN)

Fig. 2

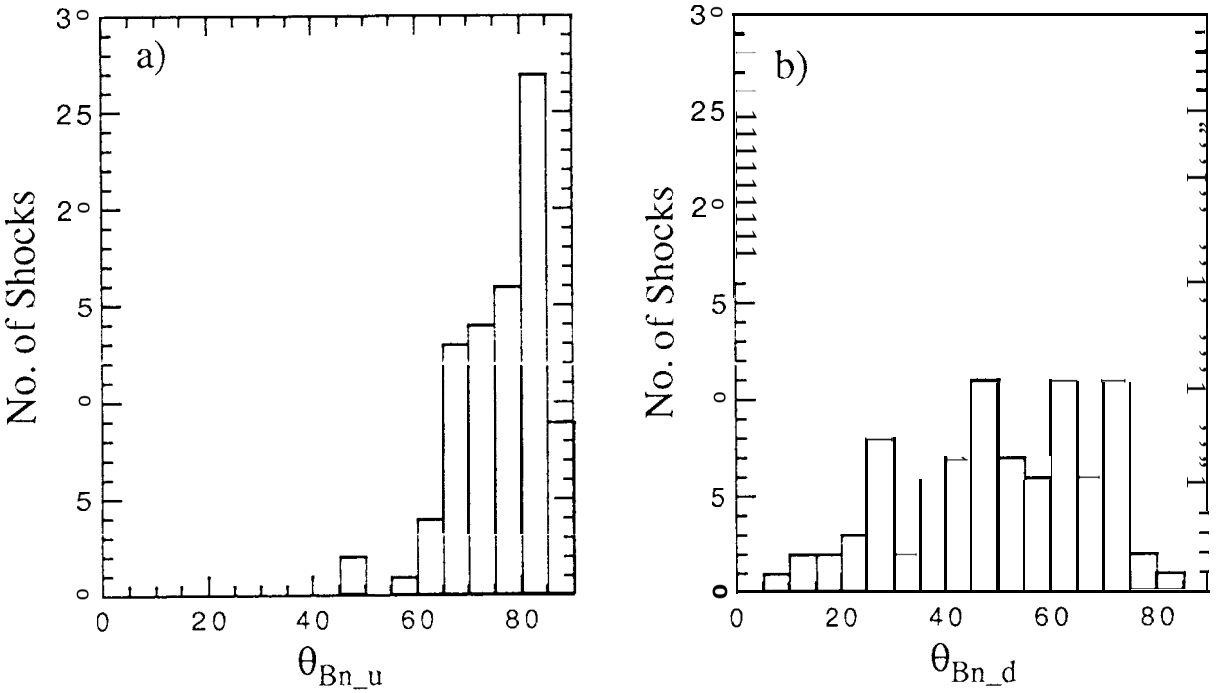

Figure 3

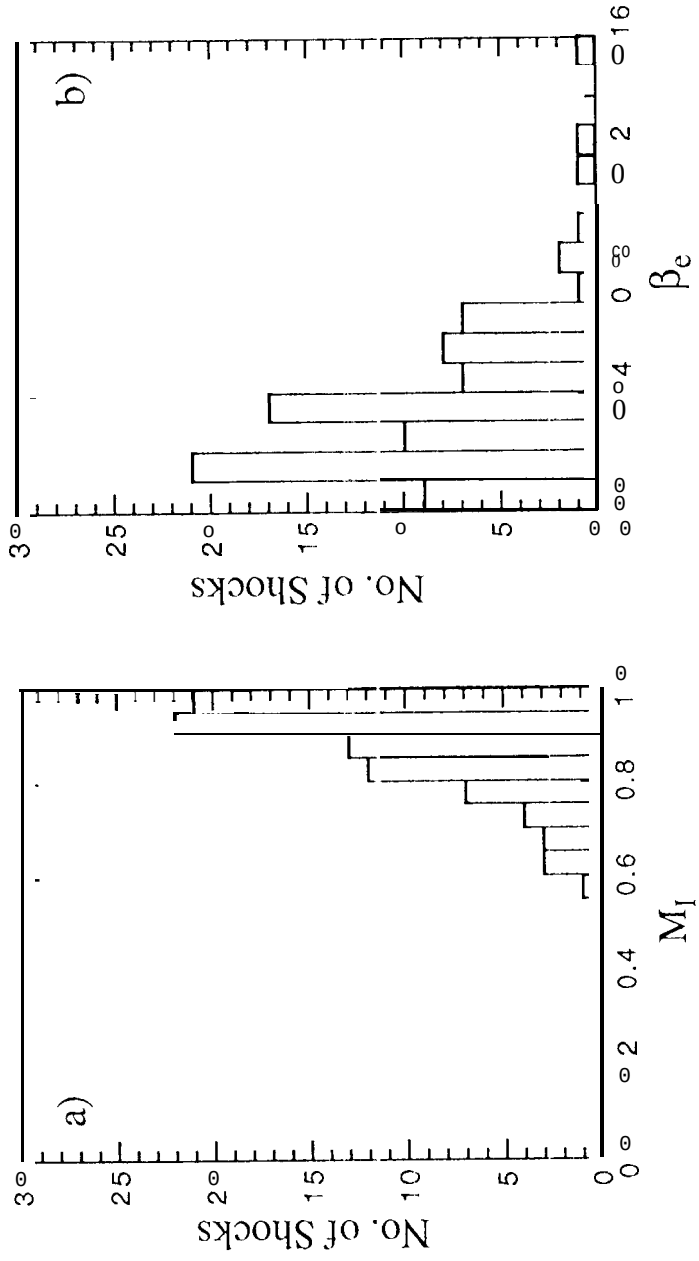
a)
No. of Shocks
0
5
10
15
20
25
30
0.0
0.2
0.4
0.6
0.8
1.0
M_I
b)
No. of Shocks
0
5
15
20
25
30
0.0
0.4
0.8
2.0
16.0
β_e

Figure 4

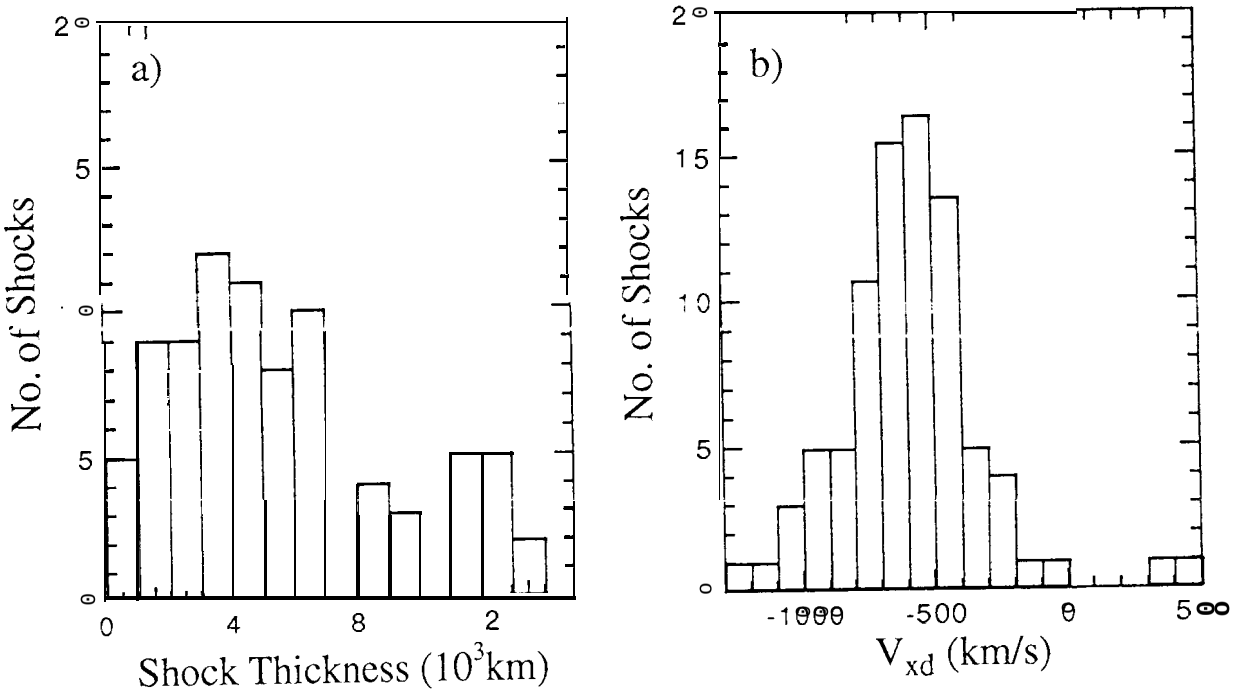

Figure 5

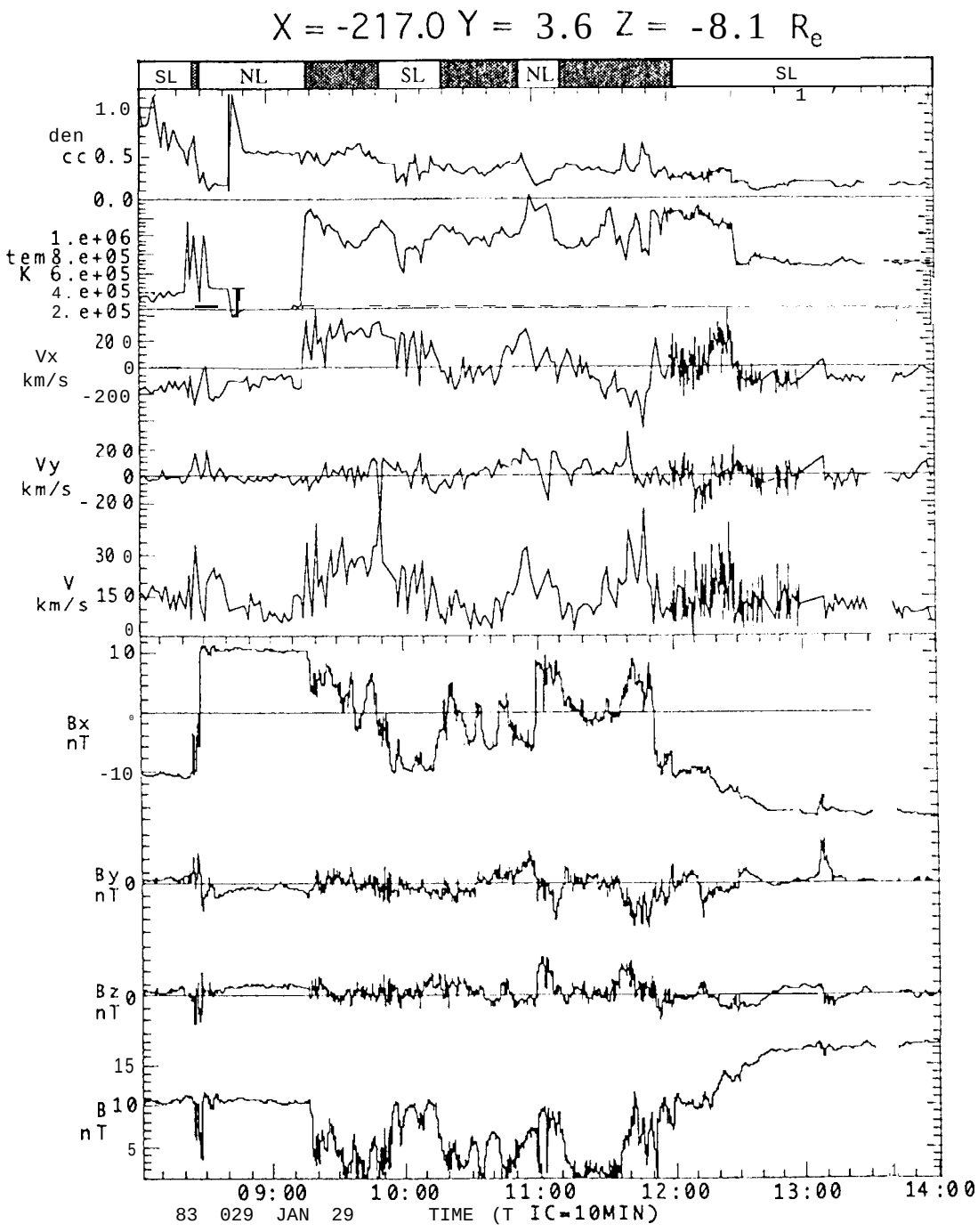
X = -217.0 Y = 3.6 Z = -8.1 Re
SL
NL
SL
NL
SL
den
cc
1.0
0.5
0.0
tem
K
1.e+06
8.e+05
6.e+05
4.e+05
2.e+05
Vx
km/s
200
0
-200
Vy
km/s
200
0
-200
V
km/s
300
150
0
Bx
nT
10
0
-10
By
nT
0
Bz
nT
0
B
nT
15
10
5
09:00
10:00
11:00
12:00
13:00
14:00
83 029 JAN 29
TIME (T IC-10MIN)

Fig. 6

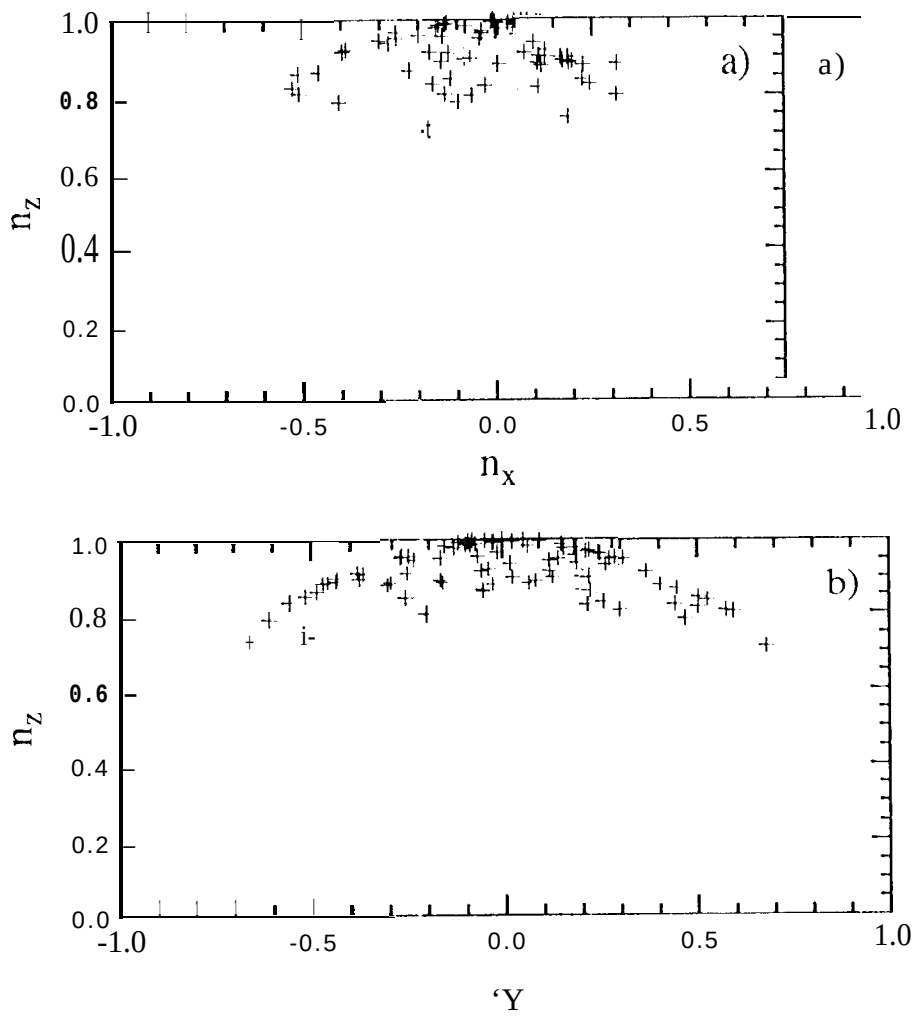
a)
a)
1.0
0.8
0.6
0.4
0.2
0.0
n_z
-1.0
-0.5
0.0
0.5
1.0
n_x
b)
1.0
0.8
0.6
0.4
0.2
0.0
n_z
-1.0
-0.5
0.0
0.5
1.0
'Y

Figure 7

IMP-8 IMF Data, Jan.17-Feb. 5 and Jun.23-Jul.22, 1983

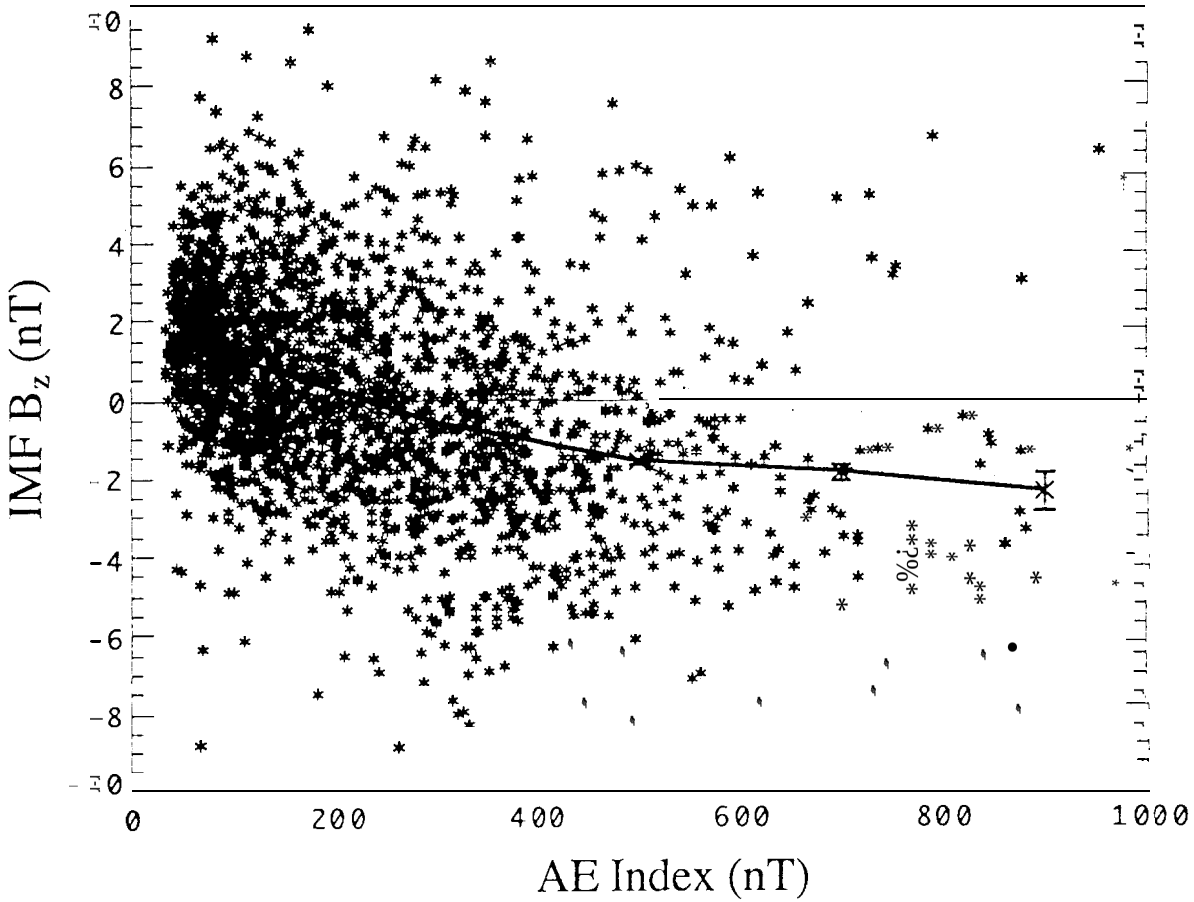

Fig 8.

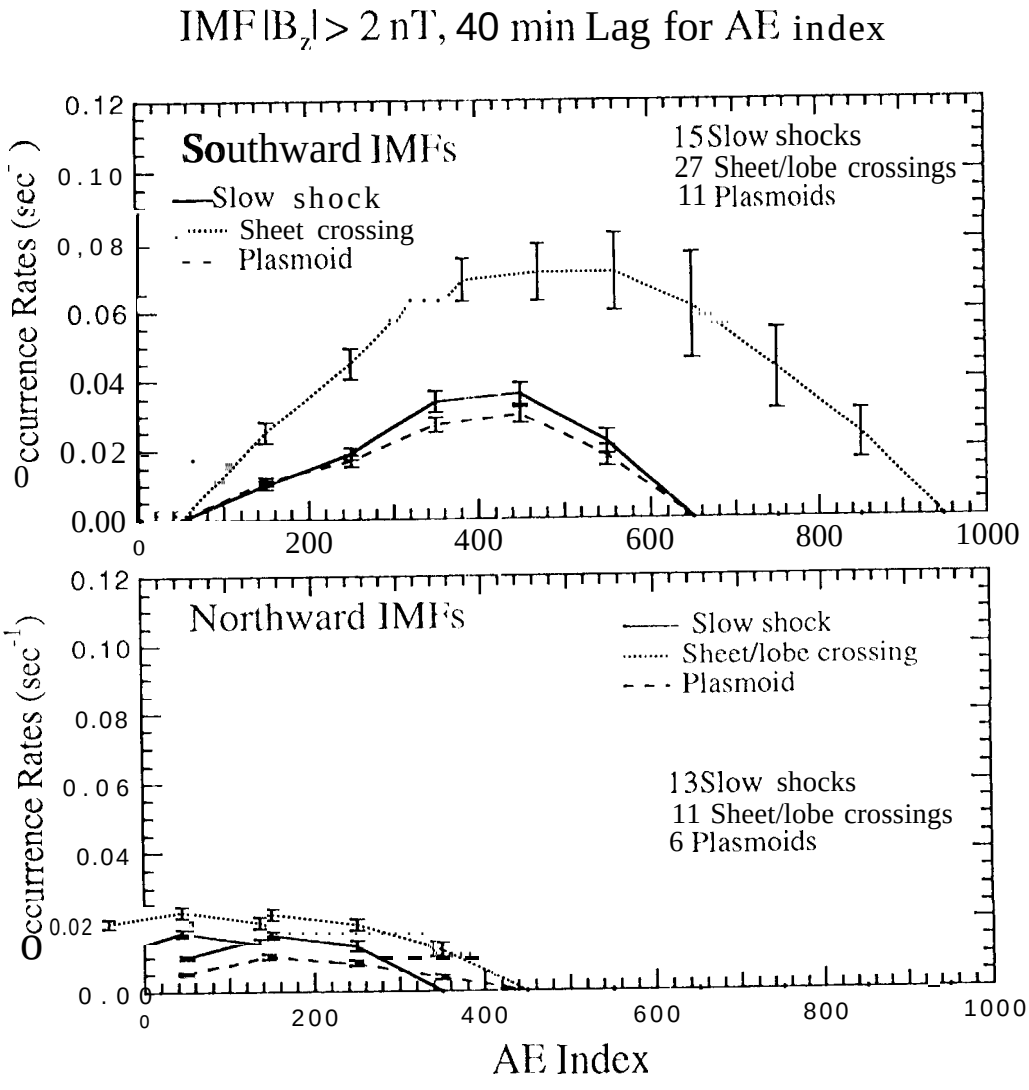
IMF $|B_z| > 2$ nT, 40 min Lag for AE index
Southward IMFs
Slow shock
Sheet crossing
Plasmoid
15 Slow shocks
27 Sheet/lobe crossings
11 Plasmoids
Northward IMFs
Slow shock
Sheet/lobe crossing
Plasmoid
13 Slow shocks
11 Sheet/lobe crossings
6 Plasmoids
Occurrence Rates (sec^{-1})
AE Index
0.12
0.10
0.08
0.06
0.04
0.02
0.00
0
200
400
600
800
1000

Figure 9

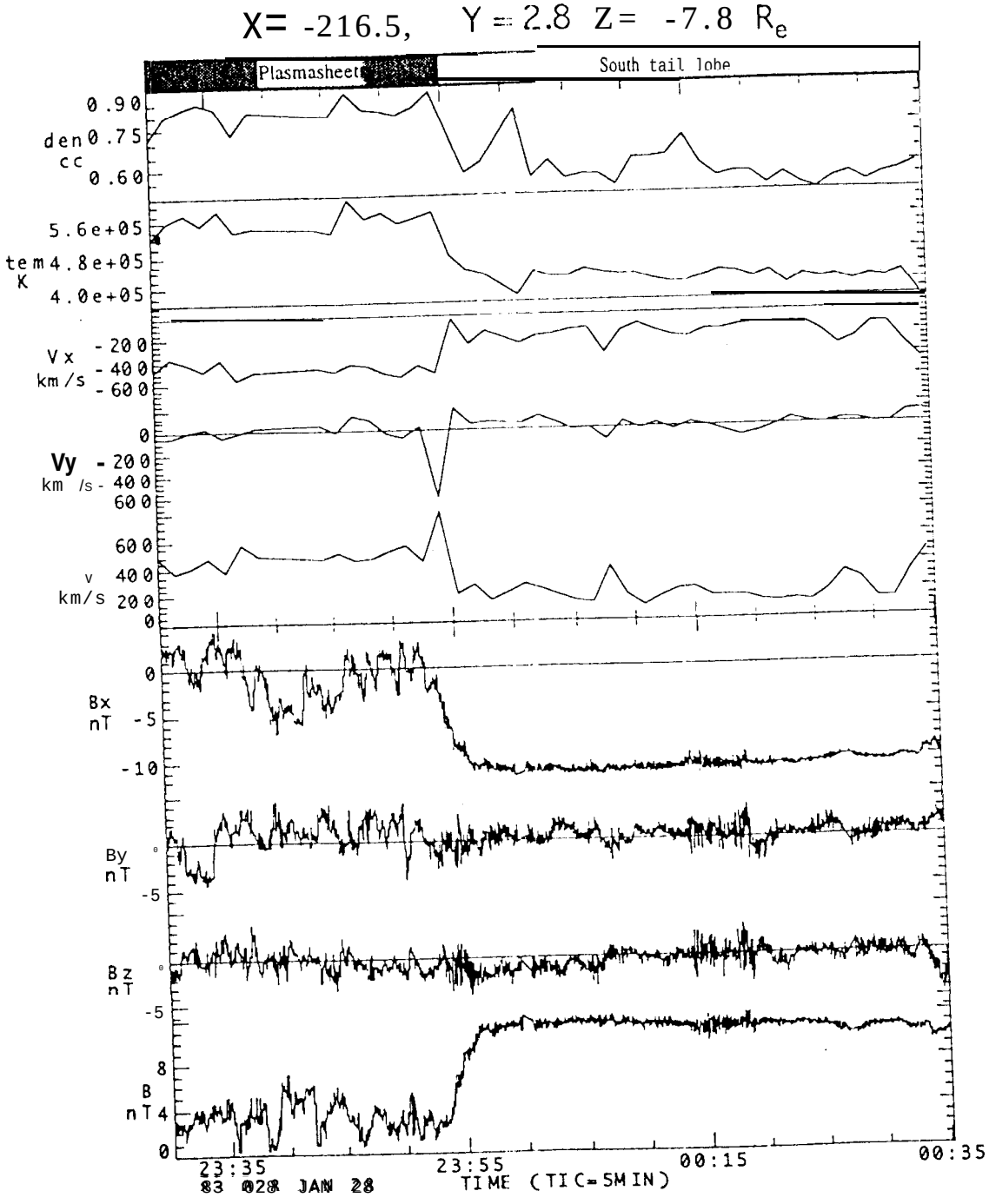
X= -216.5, Y = 2.8 Z= -7.8 R_e
Plasmasheet
South tail lobe
0.90
den 0.75
cc
0.60
5.6e+05
tem 4.8e+05
K
4.0e+05
Vx -200
km/s -400
-600
0
Vy -200
km/s -400
600
600
v 400
km/s 200
0
0
Bx -5
nT
-10
By
nT
-5
Bz
nT
-5
8
B
nT 4
0
23:35
83 028 JAN 28
23:55
00:15
00:35
TIME (TIC=5MIN)

Fig. 1